

EDGE ARTICLE

View Article Online
View Journal | View IssueCite this: *Chem. Sci.*, 2025, **16**, 10852

All publication charges for this article have been paid for by the Royal Society of Chemistry

Received 6th February 2025

Accepted 4th May 2025

DOI: 10.1039/d5sc00965k

rsc.li/chemical-science

L/Z-ligand type amphoterism of an acridinium unit†

Elishua D. Litle, Shantabh Bedajna and François P. Gabbaï*

As part of our study of ambiphilic carbenium-based ligands, we now report on the coordination chemistry of the known acridinium phosphine ligand $[(o\text{-Ph}_2\text{P}(\text{C}_6\text{H}_4)\text{Acr})]^+$ ($[\text{L}^{\text{acr}}]^+$, Acr = 9-*N*-methylacridinium) towards rhodium(I) reagents. While the simple coordination complex $[\text{L}^{\text{acr}}\text{Rh}(\text{COD})\text{Cl}]^+$ ($[\text{I}]^+$) is obtained from $[\text{L}^{\text{acr}}]^+$ and $[\text{Rh}(\text{COD})\text{Cl}]_2$ (COD = 1,5-cyclooctadiene) in CH_2Cl_2 , the use of $[\text{Rh}(\text{COE})_2\text{Cl}]_2$ (COE = cyclooctene) in MeCN affords $[(o\text{-Ph}_2\text{P}(\text{C}_6\text{H}_4)\text{Acr})\text{Rh}(\text{MeCN})_2\text{Cl}]_2^{2+}$ ($[\text{2}]_2^{2+}$), a chloride-bridged dimeric complex in which each rhodium atom is involved in a $\text{Rh} \rightarrow \text{C}_{\text{carb}}$ dative bond (C_{carb} = acridinium C9 atom), indicating Z-type behavior of the acridinium unit. The same reaction in CH_2Cl_2 affords $[(o\text{-Ph}_2\text{P}(\text{C}_6\text{H}_4)\text{Acr})\text{RhCl}]_2^{2+}$ ($[\text{3}]_2^{2+}$), a chloride-bridged dimeric square planar complex in which the acridinium assumes the role of an η^2 -heteroarene, L-type ligand. All complexes, which have been structurally characterized as their triflate salts, can be interconverted into one another *via* simple ligand exchange or displacement reactions. These experimental results, supported by computational analyses, show that the acridinium unit of $[\text{L}^{\text{acr}}]^+$ displays ligand-type amphoterism as it easily and reversibly switches from L-type to Z-type in response to changes in the coordination sphere of the metal center.

The Covalent Bond Classification (CBC) can be used to define ligands according to their ability to donate or accept electrons when interacting with a metal.¹ The extremes of this ligand classification include the most common L-type, for ligands donating two electrons to a metal, and Z-type, for ligands accepting two electrons from a metal center.^{2,3} Side-on bound arene ligands are examples of L-type ligands that contribute two electrons to the valence of a metal complex.⁴ The simplest Z-type ligands are boranes capable of accepting two electrons from a metal center.^{3,5} The diametrically opposed behavior of these two ligands can be used to modulate the electron richness of the metal center, which can be particularly useful in the context of catalysis.^{2f-h,5} However, ligands that can switch behavior from L-type to Z-type, without ligand-centered compositional changes,^{6,7} are, to our knowledge, unknown.

Our recent efforts in the chemistry of Z-type ligands has led us to consider cationic phosphines⁸ featuring a pendent carbenium functionality⁹⁻¹¹ positioned to interact with the coordinated transition metal center.¹² One of the best-studied examples of such ligands includes the cationic ambiphilic system $[\text{L}^{\text{acr}}]^+$ which features an acridinium moiety as the electron-poor unit (Fig. 1).¹⁰ Being isoelectronic with anthracene and thus aromatic, the acridinium core could, in principle, behave as an arene-like L-type ligand. While a related

behavior has been observed in the case of pyridinium units such as in $[\text{I}]^+$,¹³ the chemistry of acridinium-containing ligands is dominated by the Lewis acidity of the C9 carbon atom, referred to as C_{carb} (Fig. 1). This behavior is in full display in complexes of type $[\text{II}]^+$,¹¹ where the group 10 metal engages the acridinium unit *via* a dative $\text{M} \rightarrow \text{C}_{\text{carb}}$ interaction. Building on our interest in the design of atypical and coordination non-innocent ligands, we are now describing a series of rhodium systems in which the acridinium unit of $[\text{L}^{\text{acr}}]^+$ displays ligand amphoterism, switching its behavior from L-type to Z-type in response to changes in the coordination environment of the metal center.

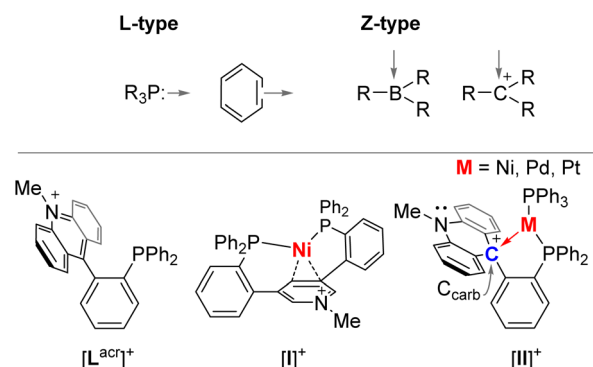


Fig. 1 Top: example of L-type and Z-type ligands. Bottom: structure of $[\text{L}^{\text{acr}}]^+$ and known complexes illustrating the L-type behavior of a pyridinium unit ($[\text{I}]^+$) and the Z-type behavior of an acridinium unit ($[\text{II}]^+$).

Department of Chemistry, Texas A&M University, College Station, TX 77843, USA.
E-mail: francois@tamu.edu

† Electronic supplementary information (ESI) available: Additional experimental and computational details and crystallographic data in cif format. CCDC 2421484–2421486. For ESI and crystallographic data in CIF or other electronic format see DOI: <https://doi.org/10.1039/d5sc00965k>



Results and discussion

Our investigation began with the reaction of $[L^{acr}][OTf]$ with $[Rh(COD)Cl]_2$ (COD = 1,5-cyclooctadiene) in CH_2Cl_2 which proceeded smoothly at room temperature to produce a new complex characterized in $CDCl_3$ by a $^{31}P\{^1H\}$ NMR resonance at 33.95 ppm split into a doublet by a $^1J_{P-Rh}$ coupling constant of 150.7 Hz (Scheme 1). This coupling is analogous to that reported for $Ph_3PRh(COD)Cl$ ($^1J_{P-Rh} = 152.0$ Hz),¹⁴ suggesting that the product of this reaction is the simple coordination complex $[L^{acr}Rh(COD)Cl][OTf]$ ($[1][OTf]$). Formation of this complex was confirmed by single crystal X-ray diffraction (see ESI†), which also shows that the acridinium ligand is disengaged from the metal and acts as a spectator unit. In agreement with this view, the $^{13}C\{^1H\}$ NMR spectrum of $[1][OTf]$ in $CDCl_3$ displays a resonance at 162.6 ppm corresponding to the uncompromised carbenium atom of $[L^{acr}]^+$. Interestingly, dissolving $[1][OTf]$ in CD_3CN results in an immediate broadening of the $^{31}P\{^1H\}$ NMR resonance, suggesting the onset of a reaction. Over time, the resonance assigned to $[1][OTf]$ disappears to give rise to a doublet at 52.95 ppm ($^1J_{P-Rh} = 128.4$ Hz), signaling the formation of a new species referred to as $[2][OTf]$ (Scheme 1). The $^1J_{P-Rh}$ coupling constant measured for $[2][OTf]$ falls within the expected range for phosphine Rh^{III} complex and can be compared to the value of 103 Hz in $RhCl_3(triphos)$.¹⁵ This new species, which assumes a dark red color in solution, also forms when $[L^{acr}][OTf]$ is allowed to react with $[Rh(COE)_2Cl]_2$ (COE = cyclooctene) in MeCN. The $^{13}C\{^1H\}$ NMR spectrum of this new complex displays a resonance at 63.02 ppm, assigned to the former carbenium center. This high field resonance indicates coordination of this center to the rhodium atom, a notion supported by the multiplicity of this signal which couples with the rhodium center *via* a $^1J_{C-Rh}$ coupling constant of 18.3 Hz. This $^{13}C\{^1H\}$ NMR chemical shift is at a higher field than that measured in the case of $[1][OTf]$ (162.6 ppm), suggesting $Rh \rightarrow C_{carb}$ dative bonding as in complexes of type $[II]^+$.¹¹

A single crystal X-ray diffraction study afforded the structure shown in Fig. 2. The rhodium atom is coordinated by four primary ligands, including two tightly bound acetonitriles, a chloride anion and the phosphine ligand. The bonds that these ligands form with the rhodium center are quite short, as

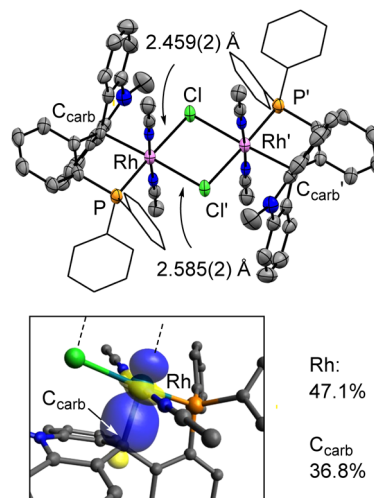
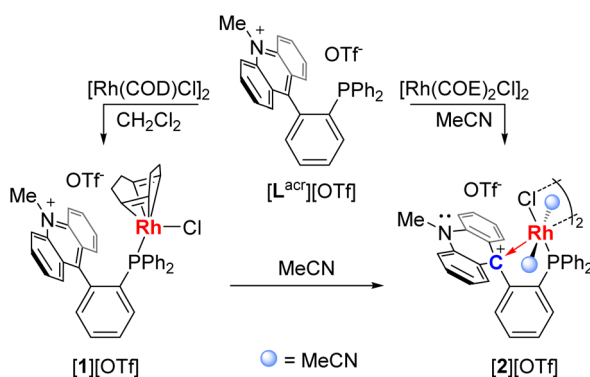


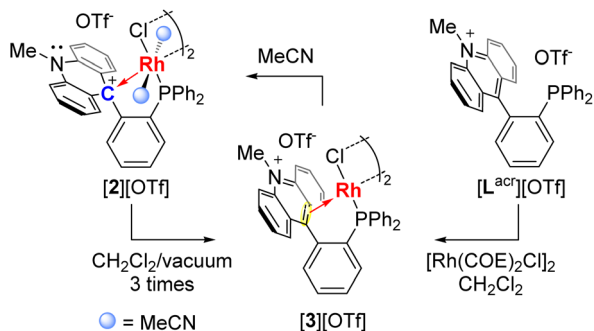
Fig. 2 Top: crystal structure of the dimeric form of $[2][OTf]$ with ellipsoid drawn at the 50% probability level. Hydrogen atoms and triflate anions are omitted for clarity. N atoms shown in blue. Bottom: truncated view of $[2]^+$ showing the Pipek–Mezey orbital defining the $Rh \rightarrow C_{carb}$ bond. The main atomic orbital parentages are also provided.

indicated by the $Rh-N$ (2.025(5) and 2.012(5) Å), $Rh-P$ (2.2301(18) Å), and $Rh-Cl$ (2.4590(16) Å) distances. These four ligands, which define a square plane, are complemented by two additional ligands positioned above and below the rhodium atom. One of these ligands is the carbenium ion of the acridinium moiety which is engaged in a long $Rh \rightarrow C_{carb}$ interaction of 2.229(6) Å with the adjacent acridinium unit. The trans site, which is acidified by the carbenium Z-type ligand,¹⁶ is occupied by the bridging chloride ligand Cl' . This bridging chloride ligand forms a $Rh-Cl'$ distance of 2.5848(16) Å which is significantly longer than the primary $Rh-Cl$ bond (2.4590(16) Å). The $Rh \rightarrow C_{carb}$ bond present in $[2][OTf]$ induces a distinct pyramidalization of the carbenium center as illustrated by the sum of the $C-C_{carb}-C$ angle of 336.4°. The polarization of the $Rh \rightarrow C_{carb}$ bond was assessed computationally through a Pipek–Mezey orbital analysis, using an approach previously adopted to probe the polarization of metal–carbon bonds.^{11,17} This analysis shows that the $Rh \rightarrow C_{carb}$ bond of $[2]^+$ displays a higher parentage from the rhodium (47.1%) than the C_{carb} carbon atom (36.8%). Altogether, the data collected for $[2][OTf]$ indicates that the acridinium unit functions as a Z-type ligand through its carbenium ion, as observed in complexes of type $[II]^+$.¹¹

Elemental analysis of $[2][OTf]$ pointed to the facile dissociation of the MeCN ligand. Intrigued by this possibility, $[2][OTf]$ was dissolved in CH_2Cl_2 and evacuated to dryness. Repeating this protocol three times produced a green solid product referred to as $[3][OTf]$ (Scheme 2). This complex is poorly soluble in CD_2Cl_2 which prevented its full characterization in this solvent. Yet, extended acquisition allowed for the detection of a $^{31}P\{^1H\}$ NMR signal at 64.71 ppm ($^1J_{P-Rh} = 135.3$ Hz), a chemical shift almost identical to that determined by ^{31}P HPDec-MAS NMR spectroscopy (63.24 ppm). An additional clue



Scheme 1 Synthesis of the rhodium complexes $[1][OTf]$ and $[2][OTf]$.



Scheme 2 Synthesis of the rhodium complex [3][OTf].

into the identity of [3][OTf] was derived from the observation that it dissolves in CD_3CN to afford [2][OTf], as confirmed by ^1H and $^{31}\text{P}\{^1\text{H}\}$ NMR spectroscopy. Further information on the nature of [3][OTf], which is also formed by reaction of [L^{acr}][OTf] with 0.5 equiv. $[\text{Rh}(\text{COE})_2\text{Cl}]_2$ in CH_2Cl_2 (Scheme 2), were obtained from an X-ray diffraction experiment (Fig. 3) carried out on single crystals obtained from a very dilute CH_2Cl_2 solution. Like its precursor [2][OTf], complex [3][OTf] exists as a chloride-bridged dimer with the rhodium atom in a distorted square planar geometry ($\tau_4 = 0.20$).¹⁸ In addition to the two bridging chloride and the phosphine ligand, the rhodium center is also coordinated in a η^2 -fashion by the flanking acridinium unit which now functions as an L-type ligand. The two carbon atoms involved in this η^2 -interaction are the carbenium center and the adjacent C_{10} atom, placing the centroid of the $\text{C}_{\text{carb}}\text{--C}_{10}$ bond at

just 2.045(3) Å from the rhodium atom. This bonding description is supported by the moderate pyramidalization of the carbenium atom ($\Sigma(\text{C}\text{--}\text{C}_{\text{carb}}\text{--}\text{C}) = 353.7^\circ$). The η^2 -interaction is rather symmetrical, as confirmed by the $\text{Rh}\text{--}\text{C}_{\text{carb}}$ and $\text{Rh}\text{--}\text{C}_{10}$ distances of 2.149(4) Å and 2.191(4) Å, respectively. These distances are close to those found in η^2 -arene rhodium(i) complexes,¹⁹ including $[\text{Cp}^*\text{Rh}(\eta^2\text{-phenanthrene})(\text{PMe}_3)]$ (III, Fig. 4) in which the arene ligand interacts with the rhodium center *via* bonds of 2.128(4) and 2.144(4) Å.²⁰ A comparison can also be made with complex [IV]⁺ which also features an intramolecular η^2 -arene coordination motif. In this case, however, the longer $\text{Rh}\text{--}\text{C}$ distance of 2.411(3) and 2.476(3) Å suggest weaker coordination of the arene ligand, possibly because of the hindrance imposed on the metal center by the norbornadiene ligand.²¹ The structure of [3][OTf] also indicates a noticeable asymmetry in the $\text{Rh}\text{--}\text{Cl}$ distances, with the longest one being formed with the chlorine atom trans to the phosphine ligand (2.4609(13) Å) and the shortest with the chlorine atom trans to the η^2 -bonded acridinium heteroarene moiety (2.3422(11) Å). A similar asymmetry is seen in $[\text{RhCl}(\text{C}_2\text{H}_4)(\text{P}^i\text{Pr}_3)]_2$ which features $\text{Rh}\text{--}\text{Cl}$ distances of 2.376(1) and 2.441(1) Å for the chlorine atom trans to the ethylene and phosphine ligand, respectively.²² These structural results support the description of [3]⁺ as a square planar rhodium(i) complex featuring an η^2 -heteroarene unit as one of the four ligands. A Pipek–Mezey orbital analysis suggests that this interaction benefits both from donation from the heteroarene π system, with significant back donation from the metal to the carbenium center (Fig. 3). An NBO calculation, carried out with full atomic disconnection, offers a consistent picture, with the forward-donation from the C_{10} carbon center to the rhodium center and the backdonation from the rhodium to the carbenium center, respectively associated with second-order energy corrections of 29.9 and 99.1 kcal mol^{−1}. These NBO results show that the backdonation dominates the η^2 -heteroarene–rhodium interaction present in this complex. The large back donation observed in this complex is typical of η^2 -arene complexes involving electron-rich transition metals.²³ Such bonding features are also seen in simple olefin complexes such as Zeise's salt for which a recent computational investigation indicates the dominant influence of the backbonding interaction.²⁴ Finally, it is worth mentioning that these interactions are asymmetrical, with the donation originating mostly from the C_{10} carbon atom while the back donation occurs between the rhodium atom and the C_{carb} atom. Such asymmetrical π -bonding and backbonding interactions are typical of polar olefin or olefin-like fragments such as borataalkenes.²⁵

The results discussed above indicate that [L^{acr}]⁺ is amphoteric (Fig. 4) in that it is able to switch its behavior from Z-type in [2]⁺ to L-type in [3]⁺, simply in response to changes in the coordination environment of the metal center. Moreover, our results show that this behavior is reversible, illustrating the versatility of this system. While ligand-type switching has been previously observed, it has, to our knowledge, always been associated with a change in the composition of the ligand.⁶ A close example of such behavior arises in the chemistry of the phosphinogermylene complex [V]⁺ which switches from Z-type

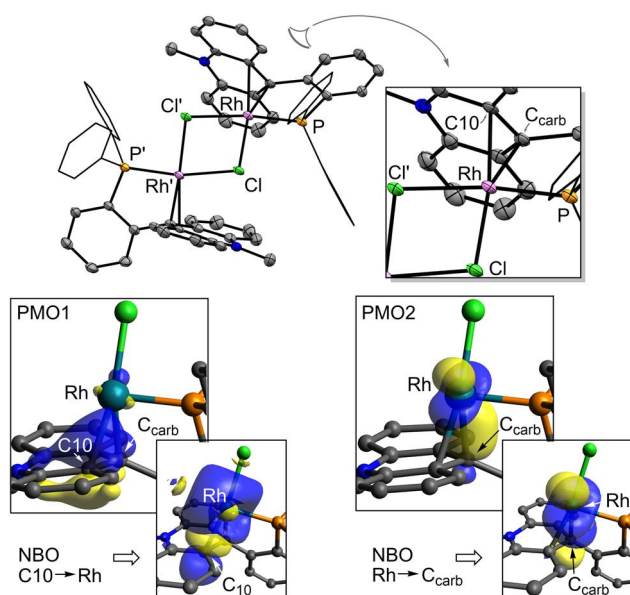


Fig. 3 Top: crystal structure of the dimeric form of [3][OTf] with ellipsoid draw at the 50% probability level. Hydrogen atoms and triflate anions are omitted for clarity. Bottom: truncated view of [3]⁺ showing the Pipek–Mezey orbitals defining the Rh–acridinium interactions (orbital parentage: PMO1: 17.0%, C_{carb} 12.3%, C_{10} 37.7%; PMO2: Rh 63.7%, C_{carb} 20.5%). The corresponding NBOs associated to the Rh–acridinium donor–acceptor bonding interactions are also shown.

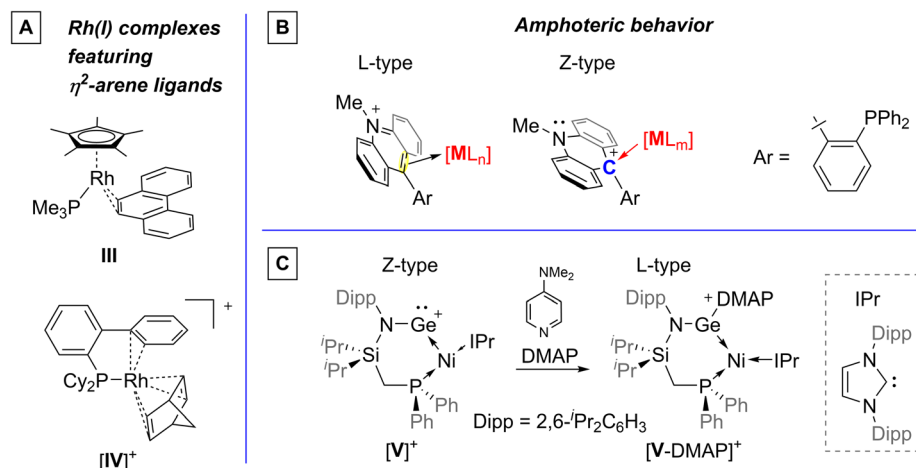
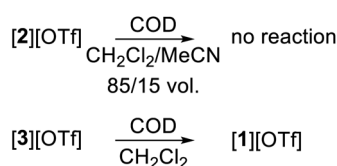


Fig. 4 (A) Examples of complexes with η^2 -arene ligands.^{19,20} (B) Amphoteric behavior of the acridinium unit of [L^{acr}]⁺. (C) A recently documented example of ligand amphoteric behavior triggered by a ligand-centered coordination event.⁷



Scheme 3 Reactions of [2][OTf] and [3][OTf] with COD.

to L-type (Fig. 4).⁷ This switch occurs upon coordination of a base to the Z-type germanium ligand, altering its composition and electronic profile. The switching behavior documented here for [L^{acr}]⁺ is thus different since it does not involve any changes in the composition of the ligand.

To conclude this study, we have also explored how changes in the ligand type would affect the reactivity of the metal center. A simple test using COD shows that [3]⁺ reacts almost immediately to form the corresponding COD complex [1]⁺ in CH₂Cl₂ (Scheme 3). To test the reactivity of [2]⁺ toward COD, we carried out an analogous experiment in which a solution of [3]⁺ in CH₂Cl₂ was first combined with MeCN (15% vol.) to ensure formation of [2]⁺ and subsequently COD, which left [2]⁺ unchanged. This lack of reactivity illustrates the ability of [L^{acr}]⁺ to alter the coordination environment and the reactivity of the metal center when switching into a Z-type ligand. The differing reactivity of [2]⁺ and [3]⁺ was further tested by investigating the behavior of these two compounds towards O₂ and H₂O, which reacted with [3]⁺ immediately to give the known phosphine oxide [(*o*-Ph₂P(O)(C₆H₄)Acrid)⁺ in the case of O₂.²⁶ As in the reaction involving COD, [2]⁺, generated *in situ* by the addition of MeCN, shows much greater robustness and remains unaffected when evaluated within 1 hour after exposure.

Conclusions

In summary, the interaction of the acridinium-phosphine ligand [L^{acr}]⁺ with [Rh(COE)₂Cl]₂ leads to different complexes, the nature of which is influenced by the conditions of the

reaction. When carried out in MeCN, this reaction affords a chloride-bridged octahedral 18-electron complex ([2]⁺) featuring two acetonitrile ligands as well as a Rh → C_{carb} donor-acceptor motif indicating that the acridinium moiety acts as Z-type ligand. The same reaction in CH₂Cl₂ follows a different course and affords a square planar complex ([3]⁺) in which the acridinium functionality behaves as a η^2 -heteroarene L-type ligand, providing two electrons to the 16-electron square planar metal center. Isolation and characterization of these two complexes highlight the amphoteric ligand behavior of the acridinium unit which can switch from L-type to Z-type based on the coordination of auxiliary ligands to the metal center. These results document a unique features of aromatic carbenium functionalities which can assume a different role in response to the electronic environment of the transition metal center. We are currently aiming to exploit these attributes in the context of catalysis.

Data availability

The data supporting this article have been included as part of the ESI.† CCDC 4 ([1][OTf]), 2421485 ([2][OTf]) and 2421486 ([3][OTf]) contains the supplementary crystallographic data for this paper.

Author contributions

Elishua D. Litle: conceptualization, data curation, investigation, methodology, writing – original draft. Shantabh Bedajna: data curation, validation, writing – original draft. François P. Gabbaï: conceptualization, data curation, funding acquisition, methodology, visualization, writing – original draft, writing – review & editing.

Conflicts of interest

There are no conflicts to declare.



Acknowledgements

We gratefully acknowledge support from the National Science Foundation (CHE-2154972) and the Welch Foundation (A-1423). All calculations were conducted with the advanced computing resources provided by Texas A&M High Performance Research Computing.

Notes and references

- 1 M. L. H. Green, *J. Organomet. Chem.*, 1995, **500**, 127–148.
- 2 (a) D. F. Shriver, *Acc. Chem. Res.*, 1970, **3**, 231–238; (b) F.-G. Fontaine, J. Boudreau and M.-H. Thibault, *Eur. J. Inorg. Chem.*, 2008, **2008**, 5439–5454; (c) J. Bauer, H. Braunschweig and R. D. Dewhurst, *Chem. Rev.*, 2012, **112**, 4329–4346; (d) R. J. Eisenhart, L. J. Clouston and C. C. Lu, *Acc. Chem. Res.*, 2015, **48**, 2885–2894; (e) J. S. Jones and F. P. Gabbai, *Acc. Chem. Res.*, 2016, **49**, 857–867; (f) R. C. Cammarota, L. J. Clouston and C. C. Lu, *Coord. Chem. Rev.*, 2017, **334**, 100–111; (g) J. Takaya, *Chem. Sci.*, 2021, **12**, 1964–1981; (h) M. T. Whited, *Dalton Trans.*, 2021, **50**, 16443–16450.
- 3 A. Amgoune and D. Bourissou, *Chem. Commun.*, 2011, **47**, 859–871.
- 4 (a) E. L. Muetterties, J. R. Bleeke, E. J. Wucherer and T. Albright, *Chem. Rev.*, 1982, **82**, 499–525; (b) J. R. Sweet and W. A. G. Graham, *J. Am. Chem. Soc.*, 1983, **105**, 305–306; (c) S. M. Hubig, S. V. Lindeman and J. K. Kochi, *Coord. Chem. Rev.*, 2000, **200–202**, 831–873; (d) G. Pampaloni, *Coord. Chem. Rev.*, 2010, **254**, 402–419.
- 5 (a) M. Devillard, G. Bouhadir and D. Bourissou, *Angew. Chem., Int. Ed.*, 2015, **54**, 730–732; (b) G. Bouhadir and D. Bourissou, *Chem. Soc. Rev.*, 2016, **45**, 1065–1079; (c) M. J. Chalkley, M. W. Drover and J. C. Peters, *Chem. Rev.*, 2020, **120**, 5582–5636.
- 6 (a) I.-S. Ke, J. S. Jones and F. P. Gabbai, *Angew. Chem., Int. Ed.*, 2014, **53**, 2633–2637; (b) J. S. Jones, C. R. Wade and F. P. Gabbai, *Angew. Chem., Int. Ed.*, 2014, **53**, 8876–8879; (c) J. Schwarzmann, T. Eskelinen, S. Reith, J. Ramler, A. J. Karttunen, J. Poater and C. Lichtenberg, *Angew. Chem., Int. Ed.*, 2024, **63**, e202410291; (d) N. Ansmann, M. Kerscher and L. Greb, *Angew. Chem., Int. Ed.*, 2025, **64**, e202417581.
- 7 A. Schulz, T. L. Kalkuhl, P. M. Keil and T. J. Hadlington, *Angew. Chem., Int. Ed.*, 2023, **62**, e202305996.
- 8 (a) J. Petušková, H. Bruns and M. Alcarazo, *Angew. Chem., Int. Ed.*, 2011, **50**, 3799–3802; (b) Y. Canac, C. Maaliki, I. Abdellah and R. Chauvin, *New J. Chem.*, 2012, **36**, 17–27; (c) C. Maaliki, C. Lepetit, Y. Canac, C. Bijani, C. Duhayon and R. Chauvin, *Chem.–Eur. J.*, 2012, **18**, 7705–7714; (d) M. Alcarazo, *Chem.–Eur. J.*, 2014, **20**, 7868–7877; (e) M. Alcarazo, *Acc. Chem. Res.*, 2016, **49**, 1797–1805; (f) K. Schwedtmann, G. Zanoni and J. J. Weigand, *Chem.–Asian J.*, 2018, **13**, 1388–1405.
- 9 (a) L. C. Wilkins, Y. Kim, E. D. Litle and F. P. Gabbai, *Angew. Chem., Int. Ed.*, 2019, **58**, 18266–18270; (b) J. Zhou, E. D. Litle and F. P. Gabbai, *Chem. Commun.*, 2021, **57**, 10154–10157; (c) G. Park, M. Karimi, W.-C. Liu and F. P. Gabbai, *Angew. Chem., Int. Ed.*, 2022, **61**, e202206265; (d) W.-C. Liu and F. P. Gabbai, *Chem. Sci.*, 2023, **14**, 277–283; (e) E. D. Litle and F. P. Gabbai, *Chem. Commun.*, 2023, **59**, 603–606.
- 10 E. D. Litle, L. C. Wilkins and F. P. Gabbai, *Chem. Sci.*, 2021, **12**, 3929–3936.
- 11 E. D. Litle and F. P. Gabbai, *Angew. Chem., Int. Ed.*, 2022, **61**, e202201841.
- 12 (a) H. Goodman, L. Mei and T. L. Gianetti, *Front. Chem.*, 2019, **7**, 365; (b) L. Mei, J. M. Veleta, J. Bloch, H. J. Goodman, D. Pierce-Navarro, A. Villalobos and T. L. Gianetti, *Dalton Trans.*, 2020, **49**, 16095–16105.
- 13 K. T. Horak, D. G. VanderVelde and T. Agapie, *Organometallics*, 2015, **34**, 4753–4765.
- 14 E. Tomás-Mendivil, R. García-Álvarez, C. Vidal, P. Crochet and V. Cadierno, *ACS Catal.*, 2014, **4**, 1901–1910.
- 15 G. G. Johnston and M. C. Baird, *Organometallics*, 1989, **8**, 1894–1903.
- 16 (a) T.-P. Lin, C. R. Wade, L. M. Pérez and F. P. Gabbai, *Angew. Chem., Int. Ed.*, 2010, **49**, 6357–6360; (b) B. R. Barnett, C. E. Moore, P. Chandrasekaran, S. Sproules, A. L. Rheingold, S. DeBeer and J. S. Figueroa, *Chem. Sci.*, 2015, **6**, 7169–7178.
- 17 S. Yogendra, T. Weyhermüller, A. W. Hahn and S. DeBeer, *Inorg. Chem.*, 2019, **58**, 9358–9367.
- 18 L. Yang, D. R. Powell and R. P. Houser, *Dalton Trans.*, 2007, 955–964.
- 19 (a) L. Cronin, C. L. Higgitt and R. N. Perutz, *Organometallics*, 2000, **19**, 672–683; (b) A. Woolf, A. B. Chaplin, J. E. McGrady, M. A. M. Alibadi, N. Rees, S. Draper, F. Murphy and A. S. Weller, *Eur. J. Inorg. Chem.*, 2011, **2011**, 1614–1625.
- 20 W. D. Jones and L. Dong, *J. Am. Chem. Soc.*, 1989, **111**, 8722–8723.
- 21 A. R. O'Connor, W. Kaminsky, D. M. Heinekey and K. I. Goldberg, *Organometallics*, 2011, **30**, 2105–2116.
- 22 A. Angelini, M. Aresta, A. Dibenedetto, C. Pastore, E. Quaranta, M. R. Chierotti, R. Gobetto, I. Pápai, C. Graiff and A. Tiripicchio, *Dalton Trans.*, 2009, 7924–7933.
- 23 L. A. Essex, A. McSkimming, N. B. Thompson, M. L. Kelty, E. A. Hill and W. H. Harman, *Organometallics*, 2020, **39**, 2545–2552.
- 24 T. Yang, Z. Li, X.-B. Wang and G.-L. Hou, *ChemPhysChem*, 2023, **24**, e202200835.
- 25 (a) Y. Yang, J. Jiang, H. Yu and J. Shi, *Chem.–Eur. J.*, 2018, **24**, 178–186; (b) M. Eaton, Y. Zhang and S.-Y. Liu, *Chem. Soc. Rev.*, 2024, **53**, 1915–1935.
- 26 W.-C. Liu, Y. Kim and F. P. Gabbai, *Chem.–Eur. J.*, 2021, **27**, 6701–6705.

